# A Posteriori Unimodality for LLM Bias Detection

Anonymous ACL submission

## Abstract

Toxicity detection is inherently subjective: what one person flags as harmful, another may consider acceptable, depending on their Socio-Demographic (SCD), yet before we can trust them as annotators we must ask: are they biased, and if so, toward whom? Undetected systematic bias in Large Language Model (LLM) annotations can propagate into downstream models and evaluations, quietly making them unreliable for the very groups they most affect. We study six widely used LLMs—ChatGPT, DeepSeek, Gemini, Mistral, Llama, and Grok—as their broad adoption makes understanding their biases particularly important. To do so, we detect and attribute polarization in human toxicity annotations to specific SCD dimensions, deriving subgroup-specific toxicity poles that serve as ground truth for measuring LLM alignment. We find that all models systematically agree with left-leaning, high-traditionalism, white and over-30 perspectives by default, while humans themselves polarize primarily along ideological rather than hereditary lines. Under Socio-Demographic Prompting (SCDP), this consensus breaks down heterogeneously: ChatGPT and DeepSeek maintain structural ideological alignment regardless of persona, while Gemini and Mistral show greater sensitivity to identity conditioning.

## 1 Introduction

Toxicity detection is often framed as a supervised classification task, where a single ground-truth label is assumed to represent the correct judgment for each text. In practice, however, toxicity is inherently subjective: annotators frequently disagree, and their judgments reflect differences rooted in SCD backgrounds (Artstein and Poesio, 2008; Uma et al., 2021; Mostafazadeh Davani et al., 2022). Rather than treating this as noise, recent work treats it as a meaningful signal (Mostafazadeh Davani et al., 2022; Uma et al., 2021). In particular, *polarization* — measured via Distance From Unimodality (DFU), which is the metric we quantify polarization in texts — distinguishes structured disagreement, where annotators split into distinct opposing groups, from variation around a shared opinion (Pavlopoulos and Likas, 2023, 2024). When annotations are collapsed into a majority label, minority perspectives are systematically erased. Sap et al. (2019) show that models trained on majority-aggregated labels are up to twice as likely to flag African American English as toxic, simply because dominant annotators encoded their norms into the gold label. Mostafazadeh Davani et al. (2022) further show that the texts most affected are precisely the socially sensitive ones. Filtering out disagreed-upon texts would remove exactly this signal, producing models accurate on average but systematically

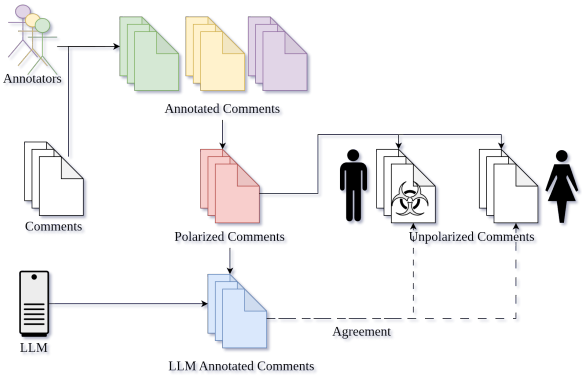


Figure 1: Using polarization we can find texts in which disagreements are caused by differences in annotator Socio-Demographic (SCD) characteristics. We use these texts to investigate which group LLM annotation prefers, in order to uncover the model's implicit "default annotator persona".

wrong for minority groups (Uma et al., 2021; Kennedy et al., 2020). This leads us to the first Research Question:

**RQ 1** *How do different social groups perceive and evaluate toxicity, and to what extent is this information lost when annotations are collapsed into a single aggregated gold label?*

Given the costs of human annotation (Rossi et al., 2024), LLMs are increasingly used for content moderation, often achieving high performance on standard benchmarks (Santurkar et al., 2023; Gallegos et al., 2024). However, the key challenge is not accuracy but whose judgment these models reflect (Santurkar et al., 2023). Trained on data dominated by majority SCD groups, LLMs learn dominant linguistic norms (Blodgett et al., 2020; Bender et al., 2021), aligning more closely with majority perspectives while diverging from less-represented ones (Sap et al., 2022; Goyal et al., 2022; Xu and Jurgens, 2026; Gallegos et al., 2024). In practice, this risks systematic over-censorship of minority communities (Sap et al., 2019; Goyal et al., 2022). We investigate these biases by answering the second research question:

**RQ 2** *How do different LLMs agree with specific subgroups that express polarized views in toxicity detection?*

Fig. 1 showcases our method. We identify polarized texts via DFU (§4.1) and apply A Posteriori Unimodality (AU) to attribute each polarized text to a specific SCD dimension: if polarization disappears within every subgroup after the division of annotations, while remaining globally present, that dimension explains it, yielding *a posteriori unimodal* texts where polarization is tied to a human subgroup (§ 4.2). We then annotate these texts with six LLMs under default prompting and SCDP (§ 4.3). Our results show that all six models systematically align with left-leaning, high-traditionalism, white, and over-30 subgroups by default, while SCDP disrupts this consensus heterogeneously across models.

## 2 Related Work

### 2.1 Annotator disagreement

Human judgments often vary in tasks that involve subjective interpretation such as detecting toxicity, hate speech, or sentiment. Early work treated this disagreement as annotation error to be corrected via majority voting or annotator filtering (Artstein and Poesio, 2008; Eijk, 2001), and early datasets typically retained only a single aggregated label for model training (Ding et al., 2025; Raza et al., 2026).

More recent work challenges this assumption, arguing that disagreement often reflects systematic differences among annotators. Mostafazadeh Davani et al. (2022) show that toxicity judgments are shaped by identity-related attributes, and that preserving individual labels allows models to capture these differences instead of collapsing them into a majority decision (Uma et al., 2021; Kennedy et al., 2020). Fornaciari et al. (2021) demonstrate that soft-label training preserves the range of annotator opinions, while Golazizian et al. (2024) propose models that explicitly incorporate annotator identity. A broader review by Uma et al. (2021) argues that disagreement is informative in socially sensitive tasks. Several studies further link this disagreement to annotator attributes (Xu and Jurgens, 2026; Goyal et al., 2022). In this work, we go further by focusing on *polarization*—cases where judgments split into distinct opposing groups rather than showing minor disagreements.

### 2.2 Sources of bias in language models

Following Gallegos et al. (2024), we define *bias* in LLMs as systematic tendencies in model outputs that favour specific social groups or perspectives in ways not justified by the task. In this work, we focus on *group-level bias*: the tendency of models to align their toxicity judgments more closely with certain SCD subgroups than others (Sap et al., 2022).

#### 2.2.1 Bias in datasets

Dataset-level bias stems from imbalances in data creation, annotation and the linguistic or cultural norms in training corpora. Toxicity datasets often encode systematic biases rather than neutral judgments. Racial and dialect disparities are documented in (Sap et al., 2019; Davidson et al., 2017; Goyal et al., 2022), with (Sap et al., 2019) showing models were up to *twice as likely* to label African American English tweets as "toxic" compared to Standard American English, even when semantically neu-

tral.

Judgments also vary with annotators' social and cultural backgrounds (Sap et al., 2022; Prabhakaran et al., 2019) and majority-vote aggregation can mask meaningful subjectivity (Kennedy et al., 2020; Röttger et al., 2021). Dataset bias is further reinforced during model training. Models absorb societal biases from large corpora (Blodgett et al., 2020; Bender et al., 2021) and training on imbalanced datasets can amplify dominant linguistic patterns (Lucy and Bamman, 2021; Sheng et al., 2021; Zhao et al., 2019; Rakshit et al., 2025), even when debiasing methods are applied.

#### 2.2.2 Bias in embeddings

Representation-level bias is well documented in both static and contextual embeddings. (Zhao et al., 2019) show that embeddings encode gender information unevenly, such as gender–career associations. Similarly, (Bolukbasi et al., 2016) find that static embeddings encode gender–occupation stereotypes and propose methods to neutralize them.

Contextual models like ELMo, BERT, and GPT-style architectures also encode structural biases: even when explicit gender directions are neutralized, hidden bias persists and affects downstream tasks (Zhao et al., 2019; Rakshit et al., 2025). Surveys (Gallegos et al., 2024) show that embedding-level bias permeates the entire model. It originates during training due to imbalanced dataset annotations and amplifies at each stage, influencing text generation, agreement, safety refusals and content moderation. This makes bias a structural issue present throughout the model pipeline.

#### 2.2.3 Prompt-induced bias

Research shows that model outputs are highly sensitive to prompt context. Small changes in framing, perspective, or identity cues can activate different parts of the model's learned distribution. Prompt-based mitigation approaches (Anantaprayoon et al., 2025) demonstrate that LLMs can produce less biased outputs when given explicit instructions discouraging stereotypes, without modifying model weights. Other studies (Perez et al., 2022; Santurkar et al., 2023) show that prompts can trigger bias, with framing shifts influencing toxicity or sentiment even without explicit personas. Work on political agreement (Santurkar et al., 2023) compares LLM outputs to survey distributions, revealing that models reflect structured ideological preferences that vary with prompt framing.

### 2.3 Polarization and polarization metrics

Polarization occurs when annotators' judgments split into distinct opposing groups, each internally consistent, rather than reflecting a shared central tendency. In subjective tasks like toxicity labeling, disagreement reflects differences in interpretation or perspective (Uma et al., 2021; Mostafazadeh Davani et al., 2022), but polarization arises only when these differences form substantial disagreement. For this reason, we focus on polarization rather than disagreement.

Agreement-based metrics convert response concentration into polarization scores (Eijk, 2001), but they are sensitive to category distances and cannot detect multiple peaks. To address this, we use the normalized DFU metric proposed in Pavlopoulos and Likas (2024), which allows polarization scores to be compared across texts with different rating distributions. DFU measures divergence from a single peak in ordinal rating histograms: multiple peaks indicate distinct annotator clusters (e.g., one group assigning consistently low scores and another consistently high scores), while a single peak reflects a convergent annotator judgment. Higher DFU values correspond to stronger polarization.

Alternative methods such as the dip test (Hartigan and Hartigan, 1985), beta-distribution-based divergence (Checco et al., 2017), and Bimodality Coefficient used in Pfister et al. (2013) provide limited or skew-sensitive estimates of polarization. Other approaches, including network analyses, experimental attitude shifts, or embedding-based classification (Garimella and Weber, 2017; Bail et al., 2018; Pereira et al., 2024), identify ideological differences but cannot differentiate between simple disagreement and structured polarization. We evaluate several polarization metrics on synthetic distributions to test their robustness; detailed results and comparisons are provided in Appendix B (see Table 6).

| #Annotators | Frequency |
|---|---|
| 1-12 | 1 |
| 4 | 122 |
| 5 | 52 |
| 6 | 450 |

Table 1: Distribution of the number of annotators per text in our dataset.

## 3 Dataset

We use the *Attitudes* dataset introduced by (Sap et al., 2022), which captures subjectivity in toxicity judgments by preserving individual annotator ratings and demographic metadata. The dataset contains 626 English social media posts, mainly from X, annotated for perceived toxicity on a 1–5 Likert scale. We chose this dataset because it retains individual ratings, allowing us to create histograms of these annotations and easily compute the polarization for each text as explained in §2.3.

Each post receives annotations from a pool of over 600 annotators, with an average of 4–6 ratings per text (see Table 1). The dataset also includes annotator attributes such as gender, race, age, political orientation, and traditionalism, allowing the study of differences in the perception of toxicity between social groups.

To preserve subjectivity, we keep the full rating distributions for each text instead of collapsing them into a single label, for the reasons explained in §1. For some analyses, scores 1–2 are treated as *civil* and ratings 3–5 are *toxic*, following (Sap et al., 2022). We retain both the original ordinal ratings (for polarization analysis) and the binary labels (for agreement comparisons). Overall toxicity statistics can be found in Fig. 2, and we include representative examples of annotated posts in Appendix C.

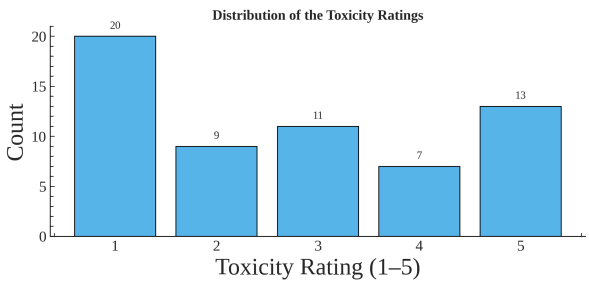


Figure 2: Distribution of toxicity ratings (1–5 Likert scale) across all annotations in the Attitudes dataset.

| Demographic | |
|---|---|
| **Gender** | **Race** |
| Women (42.3%) | White (65%) |
| Men (56%) | Black (33%) |
| Non-binary (1.7%) | Hispanic (1%) |
| | Other (1%) |
| **Age** | |
| Above 30 (58%) | |
| Below 30 (42%) | |
| **Ideological** | |
| **Politics** | **Traditionalism** |
| Far Left (14.48%) | High (60.52%) |
| Left (35.19%) | Moderate (28.19%) |
| Center (14.5%) | Low (11.29%) |
| Right (24.58%) | - |
| Far Right (8.6%) | - |

Table 2: Distribution of SCD attributes in our dataset. Percentages indicate the proportion of annotations associated with each subgroup. Underrepresented groups are excluded from certain analyses for statistical reasons.

The primary attributes examined in this study are `Gender`, `Race`, `Age`, `Traditionalism`, and `Politics`, as these capture both hereditary and ideological dimensions of annotator identity and are sufficiently represented in the dataset for meaningful subgroup analysis (Table 2). For statistical reasons, underrepresented groups (e.g., non-binary gender, very small racial subgroups) are excluded from certain analyses. We also exclude annotators associated with *moderate* traditionalism (score 3 on a 1–5 scale), as this category lacks a clear interpretive distinction.

## 4 Methodology

Our proposed framework (Fig. 3) bridges human polarization analysis with LLM evaluation through a multi-stage pipeline. Our methodology first identifies polarization in texts using the DFU metric (§2.3). We then utilize AU to attribute this polarization to specific SCD dimensions. This process yields a curated set of *a posteriori* unimodal texts where polarization is explicitly tied to a human subgroup. These texts serve as the evaluation set for six LLMs to address the study's RQs (§1).

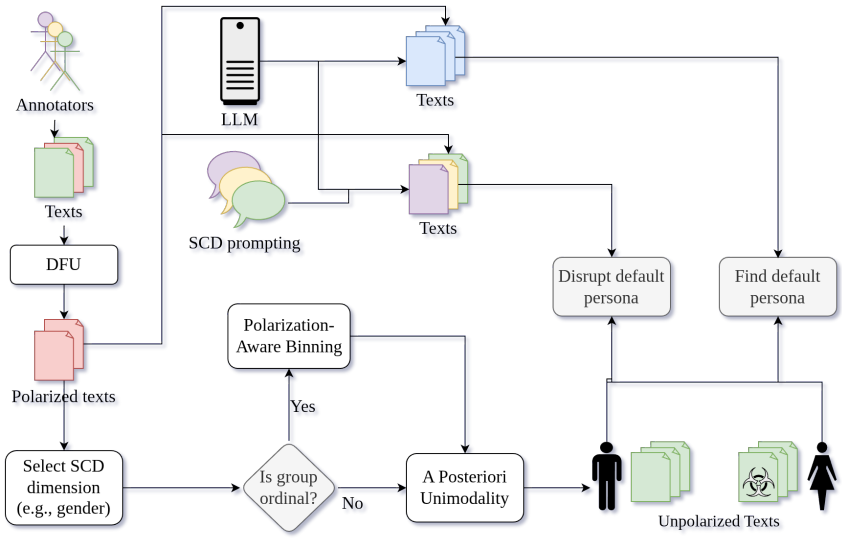


Figure 3: Overview of the polarization detection and agreement framework. The process begins by filtering the dataset for polarized texts. We apply AU to attribute polarization to SCD dimensions, including threshold-based analysis for ordinal attributes like Age. Finally, we evaluate LLM agreement with human subgroups under both **default prompting** and configurations. The latter is briefly explained in §1 but more in depth in §4.3

### 4.1 Detecting polarization

The first stage of our framework identifies texts exhibiting structured polarization. We utilize the DFU metric to quantify polarization in toxicity rating distributions (Pavlopoulos and Likas, 2023) for the reasons we outlined in §2.3. By retaining only polarized texts ($DFU > 0$), we filter out instances of insubstantial disagreement ($DFU = 0$).

### 4.2 Attributing polarization

Although DFU detects polarization, it does not reveal its source. To attribute polarization to specific annotator characteristics, we employ the AU framework (Pavlopoulos and Likas, 2024), which examines whether polarized annotation patterns are explained by contrasts between annotator groups.

**Example 4.1** *Consider the text: "Thanks to our great prime minister, haha, our homeless still sleep on the street" (Zhang et al., 2024), whose hypothetical annotations are shown in Fig. 4. It is possible that mostly poorer annotators take offense in this remark, in which case polarization is explained by economic standing.*

For each polarized text, annotations are partitioned into SCD subgroups (e.g., men vs. women for Gender). DFU is then recomputed independently for each subgroup. An SCD dimension (e.g. Gender) explains the polarization of that text if:

$$\begin{cases} DFU(X) > 0, \\ DFU(X_g) = 0 \quad \forall g \in G \end{cases}$$

where X is the set of annotation for the text and Xk is the annotations of each subgroup. G is the set of subgroups per dimension.

The text is still polarized, but if we divide annotations by each subgroup of a dimension, these subgroups become unpolarized.

**Binning.** Some attributes may be ordinal and not categorical. That is, they are provided by the dataset creators (Sap et al., 2022) in discretized values (e.g., age: 20, 25, 30). As a result, such attributes can be meaningfully partitioned either by semantics (Setlur et al., 2022) or through data-conscientious methods (Knuth, 2013). We opted for a polarization-aware binning algorithm that searches over all possible thresholds along the ordinal scale and chooses the threshold that best explains polarization (the algorithm is in Appendix D).

**Example 4.2** *If age annotations are provided in bins such as 20, 25, 30, and 35, the method evaluates all possible thresholds (e.g., $\Theta = 25, 30, 35$). A split at $\Theta = 30$ partitions annotators into those aged 30 or below ("younger") and those above 30 ("older"). Among all*

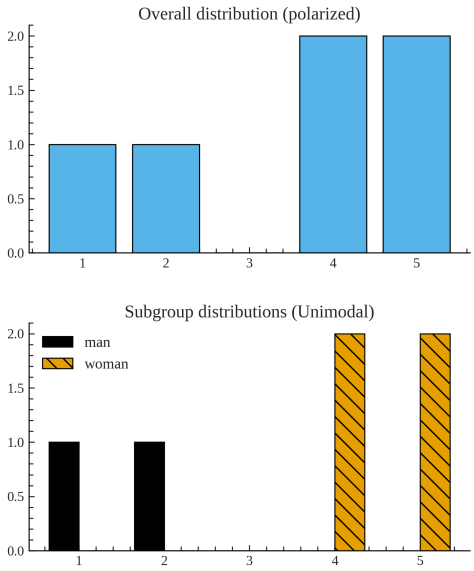


Figure 4: Example of AU attribution through distribution of ratings. The global distribution is polarized (top). After partitioning by gender (bottom), both subgroups (man vs woman) are unimodal, attributing polarization to gender.

*candidate splits, the threshold that yields the strongest attribution signal is selected, and AU is then applied to assess whether polarization disappears under this split.*

### 4.3 Comparing human with LLM annotation

After assigning a toxicity pole to each specific human subgroup (e.g., man:toxic, woman:civil), we investigate the correspondence between these groups and six LLMs: *ChatGPT*, *Gemini*, *Llama*, *Mistral*, *DeepSeek*, and *Grok* (see in Appendix E Table 9 for exact model versions). Our annotation experiments were conducted within the span of three months, although most of that time was spent on initial pilot annotations. Since all models are API-based, they required no specialized hardware (see Appendix E).

We first attempt to uncover the LLM's implicit "default" persona, which is the set of subgroups with which the LLM tends to align its toxicity judgements (see RQ2). We accomplish this with standard annotation instruction prompts without any SCD information. We then investigate whether using SCD (e.g., "Annotate as a man") can alter this alignment.

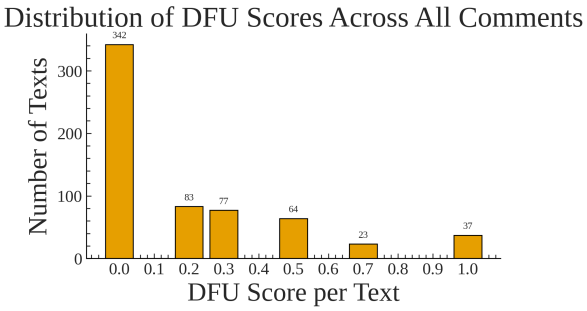


Figure 5: Distribution of DFU scores. Polarization is highly concentrated in a specific subset of the dataset.

## 5 Results

### 5.1 Ideological factors drive polarization

While 54.6% (342/626) of texts are unimodal ($DFU = 0$), a distinct subset of 284 texts exhibit structured polarization ($DFU > 0$), indicating that nearly half the dataset contains annotation patterns worth attributing to specific subgroups (Fig. 5). To study this polarization, we applied the AU framework to the polarized subset. We show a few instances of polarized texts in Appendix F; Tables 12, 13. We use data-aware binning (§4.2) to identify the optimal split.[1] We identify 10 texts in which polarization is successfully explained by Age and 92 texts where polarization is explained by a categorical dimension (Table 3).

Our analysis shows that the *polarization in human toxicity judgments is explained primarily by ideological attributes.* Traditionalism and political orientation account over more than 75% the cases attributed, while gender, race, and age explain the rest. This suggests that what divides annotators when judging toxic content is not who they are, but what they believe. This finding is consistent with previous work showing that values better explain perception of toxicity than demographic identity alone (Sap et al., 2022; Xu and Jurgens, 2026). Generally, what appears as a neutral aggregate score may, in fact, conceal a sharp ideological divide between annotator subgroups that directly answers RQ1.

Table 8 in Appendix C presents a subset of representative texts where subgroup-specific toxicity poles are observable. The full set of

[1] Specifically Strict Polarization Threshold Analysis (SPTA)—see Appendix D.1.

| Dimension | Count | % |
|---|---|---|
| Traditionalism | 57 | 55.9 |
| Politics | 20 | 19.6 |
| Age ($\Theta = 30$) | 10 | 9.8 |
| Race | 9 | 8.8 |
| Gender | 6 | 5.9 |

Table 3: Attribution of polarized texts across dimensions ($N = 102$). Ideological dimensions dominate.

| Group | Gpt | Lam | Gem | Ds | Mi | Gk |
|---|---|---|---|---|---|---|
| Man | *-29* | *-50* | *-29* | 0 | 0 | 0 |
| Woman | 22 | 45 | 22 | 0 | 0 | 0 |
| White | **80** | **80** | **60** | **60** | **60** | 20 |
| Black | *-10* | *-10* | *-9* | *-9* | *-9* | *-6* |
| F-left | **83** | 43 | **81** | **83** | **81** | **81** |
| Left | **88** | 30 | **86** | **88** | 73 | **86** |
| Center | 25 | 37 | 14 | 25 | 36 | 4 |
| Right | 16 | *-9* | 3 | 16 | 3 | 42 |
| F-right | *-21* | 23 | *-21* | *-21* | *-7* | *-21* |
| L-trad | 68 | 42 | 46 | 55 | 42 | 46 |
| H-trad | **79** | 43 | **78** | **83** | 54 | 73 |
| <30 | 0 | 0 | 0 | 0 | 0 | 0 |
| >30 | 44 | **62** | **62** | **62** | 44 | **62** |

Table 4: Cohen's $\kappa$ %-agreement between LLMs and annotator subgroups under **default prompting**. **Bold** = high agreement (≥60); *italic* = negative agreement. See Appendix E; Table 9 for the label-LLM correspondence.

102 texts provides the ground-truth for subsequent LLM agreement analysis, using the toxicity poles (e.g., `man:toxic, woman:civil`) extracted in the attribution stage. The reason why these texts can be used as ground truth is because our methodology nullifies polarization and therefore the disagreements are not substantial.

### 5.2 LLMs agree with specific human subgroups

We evaluate model agreement with polarized human subgroups using six state-of-the-art LLMs. Detailed system instructions and prompt templates for both experimental conditions and the versions of the models that were used are provided in Appendix E.

#### 5.2.1 LLMs follow the judgement of specific human groups by default

The *default prompt* condition reveals the inherent judgment of the models in the absence of identity framing in Table 4, agreement is not uniform between human groups. All models exhibit a structural agreement toward *left-leaning political perspectives*, *high-traditionalism values*, *White annotators*, and individuals *above 30 years of age*.

Agreement with certain subgroups—such as Black annotators, male annotators, or younger groups—diverges significantly from the majority-aligned trends, resulting in consistently weak or absent agreement. Some interesting facts are that of LLama that has the lowest agreement with *left and far-left* subgroups out of all models and the highest at the *far-right* subgroup. Grok has the lowest agreement out of all models with *white* annotators and the highest with *right oriented* ones. All models show moderate agreement with *low traditionalism* and strong agreement with *high traditionalism* annotators. Lastly, the models tend to agree with annotators that are *over-30*, while $\kappa$ equals zero for the *below-30* subgroup across all models, as below-30 annotators assign near-uniform labels on these polarized texts, indicating no structured alignment with any particular toxicity judgment.

#### 5.2.2 SCDP disrupts this systematic alignment

Under SCDP, models are explicitly instructed to adopt specific SCD personas when annotating each text. [2] As shown in Table 5, persona conditioning disrupts the agreement structure observed under default prompting. The previously stable cross-model consensus breaks down: the agreement becomes more heterogeneous and model-specific.

As shown in Table 5, for *political orientation*, left-leaning agreement persists in ChatGPT and DeepSeek but weakens in Llama and Mistral. Two distinct profiles emerge: ChatGPT and DeepSeek maintain strong ideological agreement regardless of persona framing, indicative of structural bias, while Gemini and Mistral exhibit greater sensitivity to identity conditioning. Notably, Llama's previously observed far-right alignment under default prompting disappears entirely, and Grok's

[2] This is not a debiasing tool, but rather a diagnostic that exposes models to direct identity frames in order to assess whether agreement patterns reflect stable internal biases or are sensitive to prompt-level framing.

| Group | Gpt | Lam | Gem | Ds | Mi | Gk |
|---|---|---|---|---|---|---|
| Man | 0 | 0 | *-67* | 0 | *-20* | 0 |
| Woman | 0 | 0 | **100** | 0 | 55 | *-15* |
| White | 25 | 0 | 75 | 25 | 75 | *-25* |
| Black | 0 | 0 | 0 | 0 | 0 | 0 |
| F-left | **100** | 32 | **83** | **64** | 49 | **64** |
| Left | **100** | 27 | 76 | **86** | 30 | 73 |
| Center | 4 | *-11* | 15 | 14 | 11 | *-20* |
| Right | 16 | 0 | 37 | 3 | *-5* | 16 |
| F-right | 0 | 0 | *-21* | *-7* | 0 | 9 |
| L-trad | 47 | 20 | **80** | 53 | 27 | 47 |
| H-trad | **65** | 16 | **65** | 52 | 57 | 5 |
| <30 | 0 | 0 | 0 | 0 | 0 | 0 |
| >30 | 29 | 29 | 58 | 29 | 29 | 44 |

Table 5: Cohen's $\kappa$ %-agreement between *SCDP-driven* LLMs and annotator subgroups. Comparison with Table 4 reveals agreement shifts relative to the default condition. **Bold** = high agreement ($\geq$60); *italic* = negative agreement.

right-leaning alignment similarly weakens, suggesting that persona conditioning disrupts these model-specific political tendencies. Overall, SCDP increases output variability without eliminating bias. Full cross-subgroup $\kappa$ results for all five dimensions under SCDP are provided in Appendix G. In the *gender* dimension, Gemini shows the most pronounced shift, with female agreement rising and male agreement dropping. *Race-based* agreement weakens across the board, with Black annotator agreement collapsing to zero under all conditions. *Age-based* agreement is the most stable dimension, with above-30 agreement persisting modestly across all models, and below-30 remaining zero. *Traditionalism* patterns are largely preserved, with Llama showing consistently low agreement across both subgroups.

## 6 Conclusion

Our results paint a consistent picture: LLMs do not approach toxicity as neutral arbiters—they carry internal perspectives that reflect the annotator demographics and ideological skews embedded in their training data. What matters is not merely that this bias exists, but that it mirrors the structure of human polarization: just as human annotators divide along ideological rather than hereditary lines, so too do LLMs align most strongly with ideological subgroups. This suggests that LLMs have internalized not just language, but the ideological divisions that shape human toxicity judgments. SCDP disrupts this structure, but does not eliminate it. That identity conditioning destabilizes inter-model consensus while leaving core ideological alignments intact in some models reveals an important distinction: some biases are surface-level and prompt-sensitive, while others are structural and resistant to framing. Understanding which is which matters enormously for anyone deploying these models in content moderation, where the cost of systematic misalignment falls disproportionately on the groups already underrepresented in training data.

Future work could extend this framework to larger datasets and intersectional subgroups, develop bias metrics tailored to polarized annotation settings and explore prompting strategies that balance competing viewpoints. A promising direction is to use LLMs directly as annotators in the same texts, compute their polarization via DFU, and compare the resulting polarization patterns and subgroup directions with those observed in human annotations. Applying the framework across additional languages and cultural contexts would also help determine whether the alignment patterns observed here generalize beyond English-language datasets.

## 7 Limitations

The *Attitudes* dataset is relatively small with low annotation density, which may affect the stability of polarization detection and subgroup attribution. After AU attribution, some dimensions retain very few texts, limiting the statistical reliability of agreement scores computed for those dimensions. The set of SCD attributes examined is also restricted—polarization that cannot be attributed through AU should not be interpreted as absence of structure, but as a limitation of the available data. Furthermore, the analysis is unidimensional, examining one attribute at a time, and does not capture intersectional effects such as race $\times$ political orientation. Finally, results are specific to the six model versions studied and should not be assumed to generalize across different releases or model families.

## 8 Ethical Considerations

This work studies bias in LLMs by exposing them to socially sensitive content including toxic and hate speech. A key ethical concern is that SCDP asks models to annotate as members of specific SCDl groups. We stress that this methodology is not recommended for standard annotation, and is used solely for diagnostic purposes in our study. Furthermore, strong model alignment with a particular subgroup should not be interpreted as that subgroup's perspective being more correct or fair—it reflects the statistical patterns present in training data. Deploying LLMs for content moderation without accounting for these alignment patterns risks systematically disadvantaging already underrepresented groups (Sap et al., 2019; Goyal et al., 2022), which is precisely the concern this work aims to surface. Finally, we stress the environmental impact of using multiple LLMs for large-scale annotation in practice. The use of multiple such models is necessary for researching the biases of these models, but is not a recommended practice for actual annotation tasks.

## References


Panatchakorn Anantaprayoon, Masahiro Kaneko, and Naoaki Okazaki. 2025. Intent-aware self-correction for mitigating social biases in large language models. *Preprint*, arXiv:2503.06011.

Ron Artstein and Massimo Poesio. 2008. Inter-coder agreement for computational linguistics. *Computational Linguistics*, 34(4):555–596.

Christopher A. Bail, Lisa P. Argyle, Taylor W. Brown, John P. Bumpus, Haohan Chen, M. B. Fallin Hunzaker, Jaemin Lee, Marcus Mann, Friedolin Merhout, and Alexander Volfovsky. 2018. Exposure to opposing views on social media can increase political polarization. *Proceedings of the National Academy of Sciences*, 115(37):9216–9221.

Emily M. Bender, Timnit Gebru, Angelina McMillan-Major, and Shmargaret Shmitchell. 2021. On the dangers of stochastic parrots: Can language models be too big? In *Proceedings of the 2021 ACM Conference on Fairness, Accountability, and Transparency*, FAccT '21, page 610–623, New York, NY, USA. Association for Computing Machinery.

Su Lin Blodgett, Solon Barocas, Hal Daumé III, and Hanna Wallach. 2020. Language (technology) is power: A critical survey of "bias" in NLP. In *Proceedings of the 58th Annual Meeting of the Association for Computational Linguistics*, pages 5454–5476, Online. Association for Computational Linguistics.

Tolga Bolukbasi, Kai-Wei Chang, James Zou, Venkatesh Saligrama, and Adam Kalai. 2016. Man is to computer programmer as woman is to homemaker? debiasing word embeddings. *Preprint*, arXiv:1607.06520.

Alessandro Checco, A. Roitero, Eddy Maddalena, S. Mizzaro, and Gianluca Demartini. 2017. Let's agree to disagree: Fixing agreement measures for crowdsourcing.

Thomas Davidson, Dana Warmsley, Michael Macy, and Ingmar Weber. 2017. Automated hate speech detection and the problem of offensive language. *Preprint*, arXiv:1703.04009.

Xiaohan Ding, Kaike Ping, Buse Çarık, and Eugenia Rho. 2025. A multi-level benchmark for causal language understanding in social media discourse. In *Proceedings of the 2025 Conference on Empirical Methods in Natural Language Processing*, pages 28776–28790, Suzhou, China. Association for Computational Linguistics.

Cees Eijk. 2001. Measuring agreement in ordered rating scales. *Quality and Quantity*, 35:325–341.

Tommaso Fornaciari, Alexandra Uma, Silviu Paun, Barbara Plank, Dirk Hovy, and Massimo Poesio. 2021. Beyond black & white: Leveraging annotator disagreement via soft-label multi-task learning. In *Proceedings of the 2021 Conference of the North American Chapter of the Association for Computational Linguistics: Human Language Technologies*, pages 2591–2597, Online. Association for Computational Linguistics.

Isabel O. Gallegos, Ryan A. Rossi, Joe Barrow, Md Mehrab Tanjim, Sungchul Kim, Franck Dernoncourt, Tong Yu, Ruiyi Zhang, and Nesreen K. Ahmed. 2024. Bias and fairness in large language models: A survey. *Computational Linguistics*, 50(3):1097–1179.

Kiran Garimella and Ingmar Weber. 2017. A long-term analysis of polarization on twitter. *Preprint*, arXiv:1703.02769.

Preni Golazizian, Alireza S. Ziabari, Ali Omrani, and Morteza Dehghani. 2024. Cost-efficient subjective task annotation and modeling through few-shot annotator adaptation. *Preprint*, arXiv:2402.14101.

Nitesh Goyal, Ian Kivlichan, Rachel Rosen, and Lucy Vasserman. 2022. Is your toxicity my toxicity? exploring the impact of rater identity on toxicity annotation. *Preprint*, arXiv:2205.00501.

J. A. Hartigan and P. M. Hartigan. 1985. The Dip Test of Unimodality. *The Annals of Statistics*, 13(1):70 – 84.

Chris J. Kennedy, Geoff Bacon, Alexander Sahn, and Claudia von Vacano. 2020. Constructing interval variables via faceted rasch measurement and multitask deep learning: a hate speech application. *Preprint*, arXiv:2009.10277.

Kevin H. Knuth. 2013. Optimal data-based binning for histograms. *Preprint*, arXiv:physics/0605197.

Li Lucy and David Bamman. 2021. Gender and representation bias in GPT-3 generated stories. In *Proceedings of the Third Workshop on Narrative Understanding*, pages 48–55, Virtual. Association for Computational Linguistics.

Aida Mostafazadeh Davani, Mark Díaz, and Vinodkumar Prabhakaran. 2022. Dealing with disagreements: Looking beyond the majority vote in subjective annotations. *Transactions of the Association for Computational Linguistics*, 10:92–110.

John Pavlopoulos and Aristidis Likas. 2023. Distance from unimodality for the assessment of opinion polarization. *Cognitive Computation*, 15(2):731–738.

John Pavlopoulos and Aristidis Likas. 2024. Polarized opinion detection improves the detection of toxic language. In *Proceedings of the 18th Conference of the European Chapter of the Association for Computational Linguistics (Volume 1: Long Papers)*, pages 1946–1958, St. Julian's, Malta. Association for Computational Linguistics.

Catarina Pereira, Raquel da Silva, and Catarina Rosa. 2024. How to measure political polarization in text-as- data? a scoping review of computational social science approaches how to measure political polarization in text-as-data? a scoping review of computational social science approaches. *Journal of Information Technology & Politics*, 22.

Ethan Perez, Saffron Huang, Francis Song, Trevor Cai, Roman Ring, John Aslanides, Amelia Glaese, Nat McAleese, and Geoffrey Irving. 2022. Red teaming language models with language models. In *Proceedings of the 2022 Conference on Empirical Methods in Natural Language Processing*, pages 3419–3448, Abu Dhabi, United Arab Emirates. Association for Computational Linguistics.

Roland Pfister, Katharina A. Schwarz, Markus Janczyk, Rick Dale, and Jonathan B. Freeman. 2013. Good things peak in pairs: a note on the bimodality coefficient. *Frontiers in Psychology*, 4:700.

Vinodkumar Prabhakaran, Ben Hutchinson, and Margaret Mitchell. 2019. Perturbation sensitivity analysis to detect unintended model biases. In *Proceedings of the 2019 Conference on Empirical Methods in Natural Language Processing and the 9th International Joint Conference on Natural Language Processing (EMNLP-IJCNLP)*, pages 5740–5745, Hong Kong, China. Association for Computational Linguistics.

Aishik Rakshit, Smriti Singh, Shuvam Keshari, Arijit Ghosh Chowdhury, Vinija Jain, and Aman Chadha. 2025. From prejudice to parity: A new approach to debiasing large language model word embeddings. *Preprint*, arXiv:2402.11512.

Shaina Raza, Mizanur Rahman, and Michael R. Zhang. 2026. Beads: Bias evaluation across domains. *Preprint*, arXiv:2406.04220.

Luca Rossi, Katherine Harrison, and Irina Shklovski. 2024. The problems of llm-generated data in social science research. *Sociologica*, 18(2):145–168.

Paul Röttger, Bertie Vidgen, Dong Nguyen, Zeerak Waseem, Helen Margetts, and Janet Pierrehumbert. 2021. HateCheck: Functional tests for hate speech detection models. In *Proceedings of the 59th Annual Meeting of the Association for Computational Linguistics and the 11th International Joint Conference on Natural Language Processing (Volume 1: Long Papers)*, pages 41–58, Online. Association for Computational Linguistics.

Shibani Santurkar, Esin Durmus, Faisal Ladhak, Cinoo Lee, Percy Liang, and Tatsunori Hashimoto. 2023. Whose opinions do language models reflect? *Preprint*, arXiv:2303.17548.

Maarten Sap, Dallas Card, Saadia Gabriel, Yejin Choi, and Noah A. Smith. 2019. The risk of racial bias in hate speech detection. In *Proceedings of the 57th Annual Meeting of the Association for Computational Linguistics*, pages 1668–1678, Florence, Italy. Association for Computational Linguistics.

Maarten Sap, Swabha Swayamdipta, Laura Vianna, Xuhui Zhou, Yejin Choi, and Noah A. Smith. 2022. Annotators with attitudes: How annotator beliefs and identities bias toxic language detection. In *Proceedings of the 2022 Conference of the North American Chapter of the Association for Computational Linguistics: Human Language Technologies*, pages 5884–5906, Seattle, United States. Association for Computational Linguistics.

Vidya Setlur, Michael Correll, and Sarah Battersby. 2022. Oscar: A semantic-based data binning approach. *Preprint*, arXiv:2207.07727.

Emily Sheng, Kai-Wei Chang, Prem Natarajan, and Nanyun Peng. 2021. Societal biases in language generation: Progress and challenges. In *Proceedings of the 59th Annual Meeting of the Association for Computational Linguistics and the 11th International Joint Conference on Natural Language Processing (Volume 1: Long Papers)*, pages 4275–4293, Online. Association for Computational Linguistics.

Alexandra Uma, Tommaso Fornaciari, Dirk Hovy, Silviu Paun, Barbara Plank, and Massimo Poesio. 2021. Learning from disagreement: A survey. *Journal of Artificial Intelligence Research*, 72:1385–1470.

Yinuo Xu and David Jurgens. 2026. Beyond consensus: Perspectivist modeling and evaluation of annotator disagreement in nlp. *Preprint*, arXiv:2601.09065.

Wenxuan Zhang, Yue Deng, Bing Liu, Sinno Pan, and Lidong Bing. 2024. Sentiment analysis in the era of large language models: A reality check. In *Findings of the Association for Computational Linguistics: NAACL 2024*, pages 3881–3906, Mexico City, Mexico. Association for Computational Linguistics.

Jieyu Zhao, Tianlu Wang, Mark Yatskar, Ryan Cotterell, Vicente Ordonez, and Kai-Wei Chang. 2019. Gender bias in contextualized word embeddings. In *Proceedings of the 2019 Conference of the North American Chapter of the Association for Computational Linguistics: Human Language Technologies, Volume 1 (Long and Short Papers)*, pages 629–634, Minneapolis, Minnesota. Association for Computational Linguistics.

## A Acronyms

**LLM** Large Language Model

**DFU** Distance From Unimodality

**AU** A Posteriori Unimodality

**SPTA** Strict Polarization Threshold Analysis

**LPTA** Lenient Threshold-Based A Posteriori Unimodality

**SCDP** Socio-Demographic Prompting

**SCD** Socio-Demographic

## B Metrics Comparison

Tests on skewed unimodal and lopsided bimodal distributions show that DFU reliably detects multimodal structures, whereas Sarle's BC (Pfister et al., 2013) and Balance (Hartigan and Hartigan, 1985), that were introduced in §2.3, often fail due to sensitivity to skew or cluster size. Agreement-based measures perform well but are limited because they depend on the distance between groups. Validation with synthetic datasets simulating edge cases common in toxicity annotations confirms DFU's robustness in distinguishing true polarization from noise or outliers.

| Metric | Unimodal | Bimodal |
|---|---|---|
| Sarle's BC | 0.5769 (Fail) | 0.9390 (Fail) |
| DFU | 0.0000 (Success) | 0.3875 (Success) |
| Agreement (A) | 0.1667 (Success) | 0.3333 (Partial) |
| Balance | 0.0000 (Success) | 0.1765 (Fail) |

Table 6: Comparison of polarization metrics on synthetic unimodal and bimodal distributions. Metric scores are shown along with success/fail interpretation.

## C Dataset Details

This table shows a few representative posts from the *Attitudes* dataset (Sap et al., 2022) with their average toxicity ratings (1–5 Likert scale). It illustrates the variability in content and perceived toxicity across posts (Table 7). **Warning: The texts contain examples of potentially harmful and offensive text included solely for scientific analysis. They do not represent the views of the authors, and we do not endorse their contents and messages.**

| Text | Tox. |
|---|---|
| I love my fam!! @Chocolatex0_ @yungboiizz @Chris2_3Black_ @KELLIS926 @SweetPeta10... | 4.17 |
| I like using words like 'nigger' or 'nigga' around black people..... | 4.50 |
| I've been to Italy a few times, and only saw two niggers in Venice... some old ... | 4.67 |
| I mean, I don't care if all the gays are infected to the nines. I'm not trying to... | 4.83 |

Table 7: Example texts and their average toxicity ratings from the Attitudes dataset. Long texts wrap to fit within a single column.

This table presents representative posts from the *Attitudes* dataset (Sap et al., 2022) corresponding to instances where the toxic poles align with specific subgroups identified through the AU analysis (Table 8). Preserving this information is crucial, as it will later enable us to measure agreement between human annotations and model predictions.

## D Data Aware Binning Algorithm

### D.1 Strict criterion

The strict strategy identifies thresholds at which polarization is fully and symmetrically explained by the attribute. A threshold is considered *strict* when both subgroups return to

Table 8: Selected AU–consolidated outputs showing subgroup toxicity poles for dimensions explaining polarization.

| **Text (excerpt)** | DFU | **Dimension** | **Poles** |
|---|---|---|---|
| Bitches be too mad bitch get some money... | 0.50 | Gender | **man**:toxic; **woman**:toxic |
| Imagine being such absolute scum, I want those south London blacks to get squashed with a roadroller | 0.25 | Race | **black**:toxic; **white**:toxic |
| #feminists disagree, for a generation that grew up with the whisper song, get low, Buble butt & bitches ain't shit... | 0.50 | Politics | **far-left**:civil; **left**:civil; **right**:toxic |
| Every police officer is a resentful son of a bitch with a lot of power | 0.67 | Traditionalism | **low**:toxic; **high**:toxic |
| Troons are worse than animals | 0.20 | Age | **below-30**:toxic; **above-30**:toxic |

unimodality:

$$DFU(A_1) = 0 \quad \text{and} \quad DFU(A_2) = 0,$$

while the global distribution remains polarized. We define the *strict AU score* as:

$$\mathrm{AU}_s = DFU(A) - \max\big(DFU(A_1),\, DFU(A_2)\big),$$

where larger values indicate stronger and more balanced restoration of unimodality across both subgroups. For a given threshold $\Theta$, we compute the meanSPTA score across all applicable texts:

$$\mathrm{MeanAU}_s(\Theta) = \frac{1}{N_\Theta} \sum_{i=1}^{N_\Theta} \mathrm{AU}_s(A_i, \Theta).$$

We retain $\Theta^*$ for which $\mathrm{MeanAU}_s(\Theta)$ is maximized, corresponding to the point where ordinal polarization is most consistently explained by the attribute. As shown in Fig. 6, this peak occurs at $\Theta^* = 30$ years, after which the AU framework is applied to the resulting subgroups.

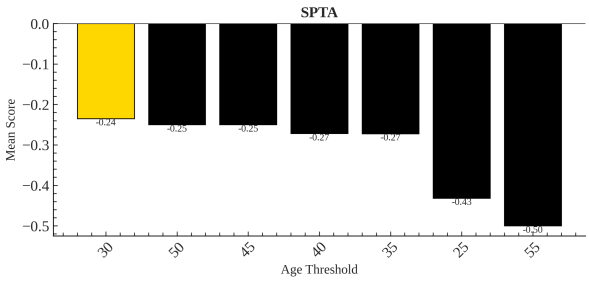


Figure 6: SPTA) across candidate age thresholds. Peaks indicate thresholds where age most strongly explains polarization.

## D.2 LPTA

To further examine age-related polarization patterns, we introduce a complementary variant of the AU framework referred to as **Lenient Threshold-Based A Posteriori Unimodality (LPTA)**. While the main body of the study relies on the SPTA, the lenient version is included here to explore *asymmetric or partially structured* polarization patterns.

The strict AU formulation requires that unimodality be restored in *both* subgroups induced by a threshold. While this ensures that polarization is fully explained by the attribute, it may exclude cases where polarization is concentrated primarily within one subgroup. Such cases can arise naturally for ordinal attributes like age, where polarization may appear directionally rather than symmetrically across groups.

The lenient formulation relaxes this requirement by allowing unimodality to be restored in *only one* of the two subgroups. Formally, given a polarized annotation distribution $A$ and a threshold $\Theta$ that partitions annotators into subgroups $A_1$ and $A_2$, the lenient AU score is defined as:

$$\mathrm{AU}_\ell = DFU(A) - \min\big(DFU(A_1),\, DFU(A_2)\big).$$

Higher values indicate a stronger reduction of polarization in at least one subgroup after conditioning.

For each candidate threshold $\Theta$, we compute the mean lenient score across all applicable texts:

$$\mathrm{MeanAU}_\ell(\Theta) = \frac{1}{N_\Theta} \sum_{i=1}^{N_\Theta} \mathrm{AU}_\ell(A_i, \Theta).$$

Fig. 7 reports MeanLPTA values across candidate age thresholds. Unlike the strict criterion, which highlights thresholds that maximize fully structured divergence, MeanLPTA identifies thresholds that minimize residual polarization within at least one subgroup. In our analysis, this minimum occurs at approximately **40 years**, suggesting that annotators above this age form a more internally consistent judgment group even when younger annotators remain polarized.

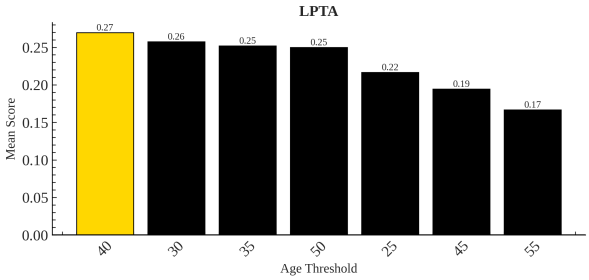


Figure 7: Mean lenient AU score (MeanLPTA) across candidate age thresholds.

Applying the lenient criterion yields **136 texts** attributed to age, compared to only **10 texts** under the strict formulation. This difference suggests that age-related polarization often manifests in a **partially structured** manner: one subgroup converges to a stable interpretation while the other remains internally diverse.

Although LPTA can reveal asymmetric polarization structures, it does not guarantee that polarization is fully explained by the attribute. For methodological consistency and interpretability, the main analysis of this study therefore relies on the strict AU formulation, while the lenient variant is included here as a complementary diagnostic analysis.

## E LLM Evaluation Prompts and Model Version

This appendix documents the exact prompts used to elicit toxicity judgments from the LLM under the two evaluation configurations described in § 4.3 and the versions of the models that where used during this study. The prompts are reported verbatim to ensure reproducibility.

**Default Prompt** In the baseline configuration, models are instructed to annotate each text without any persona conditioning. The prompt used is:

```
Analyze the following tweets
for toxicity.  Return ONLY
the score (1-5) and label
(toxic/civil) for each tweet
in this format:  score=<1-5>,
label=<toxic/civil>
```

**SCDP** In the persona-conditioned configuration, models are instructed to generate separate toxicity judgments for each specified persona within a given dimension. The prompt used is:

```
You are an annotation system.
Output ONLY valid JSON. Do not
add explanations.

Tweet:  "{tweet}"

Personas in the {dimension}
dimension:
{persona_list}

For each persona,
independently classify the
tweet as "toxic" or "civil"
and assign a score (1-5).
Each persona's judgment must
be made without considering
the judgments of the other
personas.

IMPORTANT:
- Treat each persona as a
separate and independent
annotation task.
- Do NOT ensure consistency or
comparison across personas.
- Use the persona names EXACTLY
as shown above.
- JSON keys MUST match these
personas exactly.
- Do NOT substitute or rename
personas.

Return ONLY valid JSON, for
```

```
example:
{
"{man}": {"label": "toxic",
"score": 3},
"{woman}": {"label":
"civil", "score": 1}
}
```

**Model Versions** Table 9 lists the exact version string used for each model in all experiments.

| Model | Label | Version |
|---|---|---|
| ChatGPT | gpt | gpt-4o-mini |
| Gemini | Gem | gemini-2.0-flash |
| Llama | Lam | llama-3.1-8b-instant |
| Mistral | Mi | open-mistral-7b |
| DeepSeek | Ds | deepseek-chat |
| Grok | Gk | grok-3-mini |

Table 9: LLM common names, labels used in our tables, and exact model version strings used in all experiments.

# F Dataset Statistics and Polarization Analysis

This section provides the comprehensive statistical breakdown of the dataset after DFU filtering and the threshold selection process for ordinal attributes.

## F.1 Global and dimensional DFU statistics

Table 10 summarizes the distribution of polarization across the 626 annotated texts. Approximately 45% of the dataset exhibits structured polarization ($DFU > 0$). Table 11 further breaks down these metrics across the five socio-demographic and ideological dimensions studied.

| Statistic | Value |
|---|---|
| Mean DFU | 0.205 |
| Median DFU | 0.000 |
| Standard Deviation | 0.2817 |
| Min / Max | 0.000 / 1.000 |
| $Q_1$ / $Q_3$ | 0.000 / 0.333 |
| Polarized Texts ($DFU > 0$) | 284 (45.37%) |
| Unpolarized Texts ($DFU = 0$) | 342 (54.63%) |

Table 10: Global DFU summary statistics.

| Dim. | Mean | Std | Q3 | Pol. (%) |
|---|---|---|---|---|
| Gender | 0.240 | 0.369 | 0.500 | 35.04 |
| Race | 0.279 | 0.416 | 0.500 | 34.78 |
| Age | 0.280 | 0.422 | 0.500 | 32.96 |
| Trad. | 0.257 | 0.382 | 0.500 | 36.27 |
| Pol. | 0.258 | 0.423 | 0.500 | 28.67 |

Table 11: DFU statistics across dimensions.

## F.2 Example texts before and after DFU filtering

To better illustrate how DFU operates in practice, this section presents concrete examples of texts with different DFU values prior to the application of the filtering step. Table 12 contains a small sample of texts together with their DFU scores, showing cases where the annotation distribution is either unimodal (DFU = 0) or exhibits multimodality (DFU > 0).

| Text | DFU |
|---|---|
| "you ugly bitch!!! – that seems to be my real..." | 0.0000 |
| "I am happy to report that drowning does kil..." | 0.3333 |
| "Let them praise the name of the LORD: for h..." | 0.0000 |
| "This Jestxh idiot keeps riding me in dms, t..." | 0.3333 |

Table 12: Example texts and corresponding DFU values before filtering.

The first and third texts in Table 12 receive largely consistent toxicity ratings, resulting in DFU = 0 and thus no evidence of polarization. By contrast, the remaining entries display multimodal rating patterns, reflecting polarization between annotators and therefore yielding DFU > 0. These examples highlight a key property of DFU: polarization is tied to the *shape* of the rating distribution rather than to the absolute toxicity level of a text.

Since the objective of the subsequent analysis is to study polarization and its social correlates, we retain only texts that exhibit evidence of multimodality. After filtering, the dataset consists exclusively of texts with DFU > 0, as shown in Table 13. This step ensures that downstream procedures (in particular AU attribution and model–agreement analysis) operate on cases where meaningful polarization is present.

| Text | DFU |
|---|---|
| "Fuck niggers, kikes, trannies, faggots, spics..." | 0.2000 |
| "I actually had a dream about the new MST3K co..." | 0.3333 |
| "I learned the 'bald head scaly wag' ain't go..." | 0.5000 |
| "I like to think that I have thick skin, but i..." | 0.3333 |

Table 13: Example texts after filtering (DFU > 0).

The retained texts frequently involve explicit identity references, normative claims, or morally charged content—contexts in which subjective interpretation naturally diverges. The presence of such polarization makes these items suitable candidates for subsequent *A Posteriori Unimodality* analysis, where the goal is to determine *which* subgroups contribute to the observed polarization and along *which* socio-demographic or ideological dimensions it emerges.

## G Cross-Subgroup SCDP Agreement Analysis

This appendix reports Cohen's $\kappa$ agreement scores between LLM persona-conditioned outputs and human subgroup toxicity poles across all five SCD dimensions. For each dimension we compute every ordered pair (A persona $\times$ B pole), where A is the persona adopted by the model and B is the human subgroup whose ground-truth pole is used as reference. Within-group pairs (same subgroup for persona and pole) reveal whether identity adoption recovers the corresponding human judgment; cross-group pairs expose whether a model's response under one identity inadvertently tracks a different group's perspective.

### Gender

| Pair | Gpt | Lam | Gem | Ds | Mi | Gk |
|---|---|---|---|---|---|---|
| **M → M** | **0** | **-67** | **-20** | **0** | **0** | **0** |
| M → W | 0 | 100 | 55 | 0 | 0 | 0 |
| W → M | 0 | -67 | -20 | 0 | 0 | 0 |
| **W → W** | **0** | **100** | **55** | **0** | **0** | **-15** |

Table 14: Cohen's $\kappa$ %-agreement—Gender (SCDP). **Bold** = within-group.

ChatGPT, Llama, DeepSeek, and Grok return $\kappa$=0 for every pair, indicating constant predictions regardless of persona. Gemini and Mistral are the only exceptions: Gemini reaches $\kappa$=−0.67 on both M-pole pairs and $\kappa$=1.00 on both W-pole pairs regardless of persona, systematically aligning with female ground-truth poles independently of identity framing. Mistral shows a weaker version of the same pattern ($\kappa$=−0.20 for M-pole, $\kappa$=0.55 for W-pole). Gender-based SCDP produces asymmetric rather than persona-consistent alignment.

### Race

| Pair | Gpt | Lam | Gem | Ds | Mi | Gk |
|---|---|---|---|---|---|---|
| **B → B** | **0** | **0** | **0** | **0** | **0** | **0** |
| B → W | 0 | 75 | 50 | 0 | 50 | 0 |
| W → B | 0 | 0 | 0 | 0 | 0 | 0 |
| **W → W** | **25** | **75** | **75** | **0** | **25** | **-25** |

Table 15: Cohen's $\kappa$ %-agreement—Race (SCDP). **Bold** = within-group. B = Black, W = White.

All six models return $\kappa$=0 on every Black-pole pair, regardless of persona. Agreement with the White pole is more differentiated: Gemini and Mistral achieve $\kappa$=0.75 on both W-pole pairs including the cross-group B-W pair, confirming alignment with white annotator judgments irrespective of persona. DeepSeek reaches $\kappa$=0.50 on B-W, exceeding its within-group W-W score of 0.25. Grok is the only outlier with $\kappa$=−0.25 on W-W. Overall, race-based SCDP produces majority-group alignment regardless of the adopted persona.

### Politics

The politics dimension is the richest and most heterogeneous. Three patterns stand out. First, left-leaning poles (far-left and left) attract the highest agreement scores across nearly all models and persona types. ChatGPT, Gemini, and DeepSeek achieve $\kappa \geq 0.80$ on center persona vs left pole and center persona vs far-left pole, indicating that even a centrist persona aligns strongly with left-leaning ground truth. The same holds when far-left and left personas are adopted, with perfect or near-perfect scores on left and far-left pole targets. Second, the far-right pole consistently yields negative $\kappa$ values across most models (−0.21 for ChatGPT, Gemini, DeepSeek; 0 for others), indicating systematic divergence with far-

| Pair | Gpt | Lam | Gem | Ds | Mi | Gk |
|---|---|---|---|---|---|---|
| **C-C** | **4** | **15** | **11** | **-11** | **14** | **-20** |
| C-FL | 100 | 83 | 49 | 32 | 58 | 100 |
| C-FR | -21 | -21 | 0 | 0 | -21 | 0 |
| C-L | 100 | 76 | 30 | 27 | 69 | 86 |
| C-R | 28 | 37 | -5 | 32 | 16 | 28 |
| **FL-FL** | **100** | **83** | **49** | **32** | **64** | **64** |
| FL-C | 4 | 15 | 11 | -11 | 25 | 25 |
| FL-FR | -21 | -21 | 0 | 0 | -21 | -21 |
| FL-L | 100 | 76 | 30 | 27 | 73 | 73 |
| FL-R | 28 | 37 | -5 | 32 | 28 | 28 |
| **FR-FR** | **0** | **-21** | **0** | **0** | **-7** | **9** |
| FR-C | 0 | 15 | 31 | 0 | -28 | -68 |
| FR-FL | 32 | 83 | 65 | 0 | 64 | -21 |
| FR-L | 27 | 76 | 45 | 0 | 47 | -22 |
| FR-R | -14 | 37 | 3 | 0 | 3 | 15 |
| **L-L** | **100** | **76** | **30** | **27** | **86** | **73** |
| L-C | 4 | 15 | 11 | -11 | 4 | 25 |
| L-FL | 100 | 83 | 49 | 32 | 81 | 64 |
| L-FR | -21 | -21 | 0 | 0 | -21 | -21 |
| L-R | 28 | 37 | -5 | 32 | 42 | 28 |
| **R-R** | **16** | **37** | **-5** | **0** | **3** | **16** |
| R-C | -11 | 15 | 11 | 0 | -11 | -42 |
| R-FL | 58 | 83 | 49 | 0 | 81 | 49 |
| R-FR | 0 | -21 | 0 | 0 | 0 | 44 |
| R-L | 50 | 76 | 30 | 0 | 69 | 38 |

Table 16: Cohen's $\kappa$ %-agreement—Politics (SCDP). **Bold** = within-group. FL = Far-Left, L = Left, C = Center, R = Right, FR = Far-Right.

right annotator judgments regardless of persona. Third, Llama returns $\kappa$=0 on almost all pairs, reflecting the variance collapse seen in other dimensions. Grok is the most erratic, posting $\kappa$=−0.68 on far-right persona vs center pole alongside an anomalously high $\kappa$=0.44 on far-right persona vs far-right pole which is the highest within-group far-right score among all models.

### Traditionalism

| Pair | Gpt | Lam | Gem | Ds | Mi | Gk |
|---|---|---|---|---|---|---|
| **H-H** | **65** | **65** | **57** | **16** | **52** | **5** |
| H-L | 57 | 80 | 45 | 10 | 23 | -21 |
| L-H | 54 | 65 | 34 | 33 | 54 | 39 |
| **L-L** | **47** | **80** | **27** | **20** | **53** | **47** |

Table 17: Cohen's $\kappa$ %-agreement—Traditionalism (SCDP). **Bold** = within-group. H="High", L="Low".

Traditionalism yields computable $\kappa$ across all pairs. ChatGPT and Gemini achieve strong high-high agreement ($\kappa$=0.65), with Gemini's anomalous high-low score ($\kappa$=0.80) suggesting its high-traditionalism persona tracks low-traditionalism labels better than the intended target. Llama underperforms across all pairs (max $\kappa$=0.33). Grok inverts: low-high cross-group agreement (0.39) alongside negative high-low (−0.21), indicating a contrastive rather than assimilative response to identity framing. DeepSeek is the most consistent (0.52–0.54 on three pairs).

### Age

| Pair | Gpt | Lam | Gem | Ds | Mi | Gk |
|---|---|---|---|---|---|---|
| >-> | **29** | **58** | **29** | **0** | **29** | **44** |
| >-< | 0 | 0 | 0 | 0 | 0 | 0 |
| <-> | 29 | 58 | 29 | 0 | 29 | 29 |
| <-< | **0** | **0** | **0** | **0** | **0** | **0** |

Table 18: Cohen's $\kappa$ %-agreement—Age (SCDP). **Bold** = within-group. >: more than 30, <: less than 30.

All <30 pairs return $\kappa$=0 across all models. Above-30 agreement is led by Gemini ($\kappa$=0.58), Grok (0.44), and ChatGPT, Mistral, DeepSeek (0.29 each); Llama remains zero throughout. Critically, >30 and <30 persona scores are identical for all models, confirming that persona conditioning has no differential effect on age-based agreement and that the above-30 pull is a stable internal tendency resistant to identity framing.

## H Pairwise Inter-Model Agreement

This appendix section reports pairwise Cohen's $\kappa$ and Pearson correlation between all six LLMs pairs under both default and SCDP prompting conditions. The goal is to assess whether models converge toward a shared judgment profile or exhibit distinct response patterns, and whether identity conditioning disrupts or preserves inter-model consistency.

### H.1 Default prompting

Fig.s 8 and 9 report pairwise agreement between model outputs under default prompting, measured by Cohen's $\kappa$ and Pearson correlation respectively. The $\kappa$ matrix reveals that ChatGPT and DeepSeek are the most tightly coupled pair ($\kappa$=0.86), followed by DeepSeek–Gemini (0.85) and ChatGPT–Gemini (0.76), suggesting these three models share a similar internal judgment structure. Grok aligns moderately with the same cluster (0.69–0.79), while

Llama is the most divergent model, achieving the lowest pairwise scores across all comparisons (0.44–0.53). Mistral occupies an intermediate position, agreeing more strongly with the ChatGPT–DeepSeek–Gemini cluster (0.59–0.68) than with Llama (0.39).

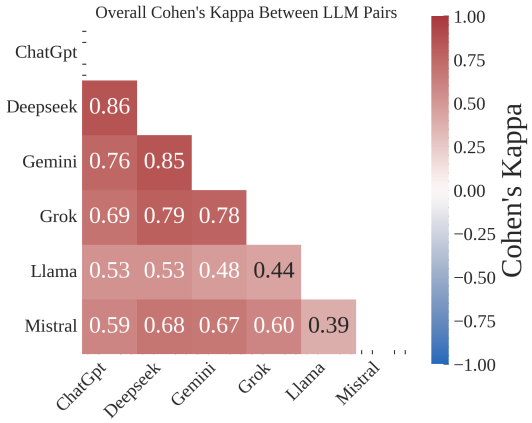


Figure 8: Pairwise Cohen's $\kappa$ between all six LLM pairs under default prompting.

The Pearson correlation matrix largely mirrors this structure but with uniformly higher values, reflecting that continuous score agreement is stronger than label agreement. ChatGPT–DeepSeek again leads (0.86), with the same top cluster intact. Grok's Pearson scores are notably higher than its $\kappa$ scores (0.72–0.81 vs. 0.69–0.79), while Llama remains the most divergent model (0.51–0.56). Mistral–Llama remains the weakest pair under both metrics ($\kappa$=0.39, $r$=0.41), confirming that these two models represent the most distinct judgment profiles in the default prompting condition.

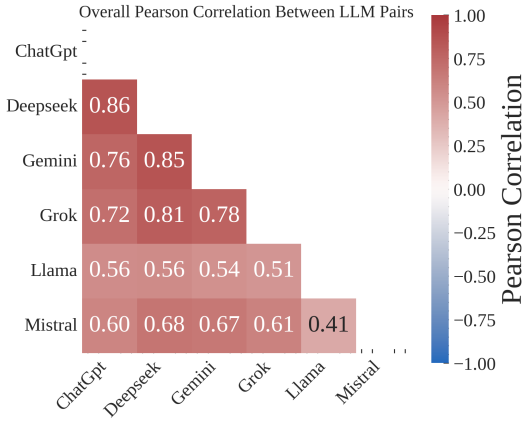


Figure 9: Pairwise Pearson correlation between all six LLM pairs under default prompting.

## SCDP

Fig.s 10 and 11 report pairwise agreement between model outputs under SCDP, measured by Cohen's $\kappa$ and Pearson correlation respectively. The $\kappa$ matrix reveals a marked drop in inter-model consistency relative to default prompting. ChatGPT–DeepSeek remains the strongest pair ($\kappa$=0.76), but all other scores decline substantially, with Grok–Gemini (0.23) and Mistral–Grok (0.13) becoming the weakest pairs. Llama, which was the most divergent model under default prompting, now aligns more strongly with ChatGPT (0.73) and DeepSeek (0.63), suggesting that identity conditioning partially reorients its outputs toward the dominant cluster. Grok and Mistral become the most isolated models, with Grok showing consistently low agreement across all pairs (0.13–0.40).

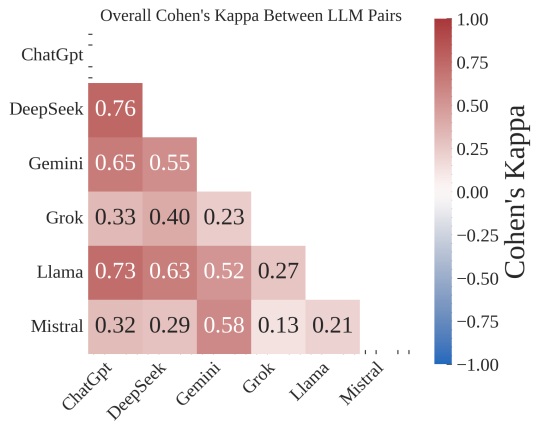


Figure 10: Pairwise Cohen's $\kappa$ between all six LLM pairs under SCDP.

The Pearson correlation matrix shows a similar collapse in consistency, with values uniformly lower than under default prompting. ChatGPT–DeepSeek drops sharply to 0.56, and Grok again anchors the weakest pairs (Grok–ChatGPT 0.24, Grok–Mistral 0.15). Gemini–Mistral is the strongest Pearson pair not involving the top cluster (0.65), suggesting some score-level alignment between these two models under persona conditioning. Overall, SCDP substantially reduces inter-model agreement, confirming that identity framing introduces model-specific response patterns that break the shared judgment structure observed under default prompting.

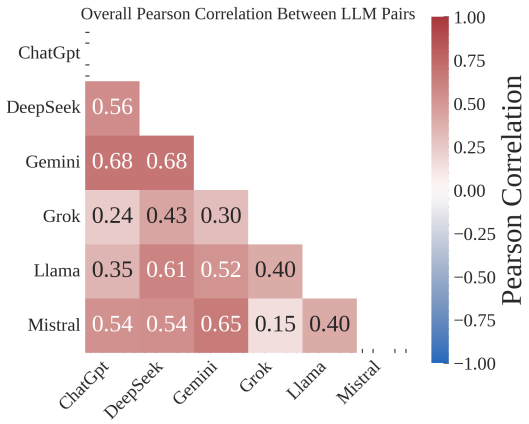


Figure 11: Pairwise Pearson correlation between all six LLM pairs under SCDP.